ACS OMEGA

Open Access

http://pubs.acs.org/journal/acsodf

Article

Temperature-Induced Luminescence Intensity Fluctuation of Protein-Protected Copper Nanoclusters: Role of Scaffold Conformation vs Nonradiative Transition

Anna Sebastian, Kavya P, Aarya, and Supratik Sen Mojumdar*

Cite This: *ACS Omega* 2024, 9, 21520−21527

Read Online

ACCESS | Metrics & More | Article Recommendations | Supporting Information

ABSTRACT: Protein-scaffolded atomically precise metal nanoclusters (NCs) have emerged as a promising class of biofriendly nanoprobes at the forefront of modern research, particularly in the area of sensing. The photoluminescence (PL) intensity of several nanoclusters showed a systematic temperature-dependent fluctuation, but the mechanism remains ambiguous and is poorly understood. We tried to shed some light on this mechanistic aspect by testing a couple of hypotheses: (i) conformational fluctuation of the protein scaffold-mediated PL intensity fluctuation and (ii) PL intensity fluctuation due to the variation in the radiative and nonradiative transition rates. Herein, the PL intensity of the lysozyme-capped copper nanocluster (Lys-Cu NC) showed excellent temperature dependency; upon increasing the temperature, the PL intensity gradually decreased. However, contrasting effects can be seen when the nanocluster is exposed to a chemical denaturant (guanidine hydrochloride (GdnHCl)); the PL intensity increased with the increase in the GdnHCl concentration due to the change in the ionic strength of the medium. This discrepancy clearly suggests that the thermal PL intensity fluctuation cannot be explained by a change in the scaffold conformation. Furthermore, upon closer investigation, we observed a 2-fold increase in the nonradiative decay rate of the Lys-Cu NC at the elevated temperature, which could reasonably explain the decrease in the PL intensity of the nanocluster at the higher temperature. Additionally, from the result, it was evident that the protein scaffold−metal core interaction played a key role here in stabilizing each other; hence, the scaffold structure remained unaffected even in the presence of chemical denaturants.

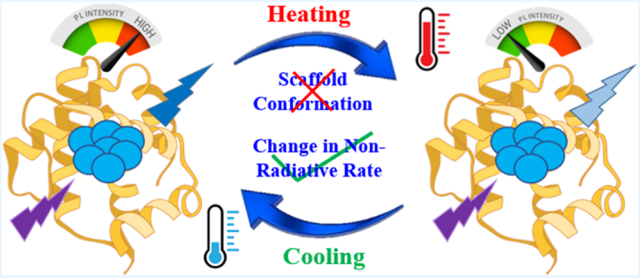

1. INTRODUCTION

Noble metal nanoclusters have emerged as a superior class of luminescent nanoprobes with a wide range of interdisciplinary applications.[1−3] The photoluminescence properties have been assigned to the ultrasmall size of the nanoclusters, comparable to the Fermi wavelength (∼2 nm) of electrons, enabling them to possess molecule-like properties with discrete energy levels.[1−3] Moreover, they exhibit excellent physicochemical properties like biocompatibility,[4,5] size-tunable emission,[6] better water solubility,[7] and robust photostability.[4,5,8] These exceptional features make them preferred alternatives to traditional fluorophores like toxic quantum dots and organic dyes.[9,10] Metal NCs comprise an inorganic metal core and an organic ligand shell.[1,11] Ligands play a pivotal role in shaping up the nanocluster by preventing zerovalent cluster cores from forming bigger-sized nanoparticles through their aggregation.[12] Apart from stabilization, the photophysical and morphological properties of NCs as well as their applications can be efficiently tuned by varying the nature of the surface ligands used during their fabrication.[13]

To date, a wide variety of scaffolds such as proteins,[5,8] peptides,[14,15] DNA,[16,17] polymer,[18] dendrimers,[19] amino acids,[20−22] etc. have been extensively used for the facile synthesis of noble metal NCs. Among them, proteins were widely used due to the availability of a large number of functional groups (such as $-NH_2$, −COOH, −OH, −SH, etc.) in the side chains that can swiftly coordinate and stabilize the metal core.[23] Recent reports showed that the photoluminescence intensity of the protein-scaffolded metal nanoclusters can be varied systematically by altering the temperature of the medium. The photoluminescence intensity of the lysozyme-capped Cu nanocluster is shown to vary linearly and reversibly upon changing the temperature of the medium.[5] Similar trends have also been reported for other protein-protected metal nanoclusters.[8,24−27] In all of these cases, the PL intensity of the nanocluster decreased upon increasing the temperature of the medium, suggesting a common mode of action. In general, the

Received: March 6, 2024
Revised: April 3, 2024
Accepted: April 23, 2024
Published: May 1, 2024

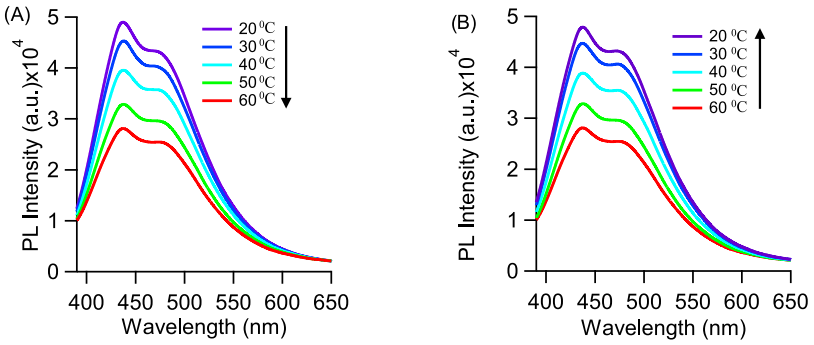

Figure 1. Temperature-dependent systematic PL intensity variation for Lys-Cu NC (λ_{ex} = 365 nm) (A) ascending from 20 to 60 °C and (B) descending from 60 to 20 °C.

findings collectively demonstrate the sensitivity of the PL intensity of the protein-protected metal NCs toward the surrounding temperature of the medium and thus can potentially be used as a temperature sensor.

Temperature is well-known as a common denaturant leading to the fluctuation of protein conformation. Under higher temperatures, most of the proteins denature and attain the unfolded conformation.[28−30] Consequently, the conformation of the protein scaffold has been hypothesized to be playing a key role in the variation of the PL intensity of the nanoclusters.[5,8,24−27,31−35] In contrast, the PL intensity of several other small ligand-capped metal nanoclusters also showed a similar temperature dependency, making this hypothesis ambiguous and elusive, particularly in the absence of any concrete evidence.[36−40] Thus, this conflict eventually opens up the necessity of a detailed investigation into the role of protein scaffold conformation in the PL intensity of metal nanoclusters in detail.

In this study, we tried to shed some light on this aspect by investigating the effect of chemical denaturants (GdnHCl and urea)[41,42] on the PL intensity of the protein-protected metal nanoclusters. We have chosen lysozyme-protected Cu NC as the potential system for these studies since the PL intensity of this nanocluster has been reported to be extremely sensitive toward temperature.[5] By comparison of the results obtained by chemical denaturation to that of the temperature-dependent PL intensity variation of the Lys-Cu NC, a detailed mechanistic insight can be gained. Protein denaturation is a process in which the protein undergoes conformational changes by losing its tertiary and secondary structures in the presence of the denaturant. For small molecules or single amino acids, this effect should be neutralized. Thus, the L-tryptophan-capped copper nanocluster (Trp-Cu NC) has been used as a negative control in this study since the PL intensity of this nanocluster should not be affected by any conformational transition of the scaffold.

Here, we observed a similar trend for both the Lys-Cu NC and the Trp-Cu NC when subjected to denaturation conditions, suggesting that the protein conformation does not impact the PL properties of the nanoclusters significantly. The chemical denaturant-induced marginal alteration in the PL intensity of the NC can primarily be attributed to changes in the ionic strength of the surrounding environment. The results indicate a mutual cooperative interaction between the protein scaffold embedded on the surface of the nanocluster and the metal core; the protein scaffold stabilizes the metal core, and in turn, the metal core provides structural support to the protein scaffold, making the protein backbone stiffer. Thus, a fluctuation in the protein conformation as a possible reason for the thermal PL intensity variation can be discarded. Further studies revealed that the substantial variation in the radiative and nonradiative rates upon changing the temperature can be attributed to the temperature-dependent PL intensity fluctuation of the nanocluster. Henceforth, this study can enhance the comprehension regarding the effect of scaffold conformation on the PL properties of the protein-capped metal nanoclusters and thereby pave the pathway for a better understanding of protein−metal interactions under various environments.

2. RESULTS AND DISCUSSION

The synthesized lysozyme-capped copper nanocluster (Lys-Cu NC) showed excellent photoluminescence (PL) properties. When excited at 365 nm, the nanocluster showed a strong PL intensity centered around 437 nm with utmost stability.[43] Upon comparison of the PL intensity of the nanocluster with the pure lysozyme exposed to the same reaction conditions, it is evident that the PL intensity is the inherent characteristic of the metal core and does not come from the protein scaffold when excited at 365 nm (Figure S1). The temperature-dependent PL intensity fluctuation of the synthesized Lys-Cu NC was first confirmed, and the PL intensity of the nanocluster indeed varied as a function of temperature. Upon increasing the temperature from 20 to 60 °C, the PL intensity of the Lys-Cu NC gradually decreased. Conversely, the PL intensity increased and was completely restored upon decreasing the temperature from 60 to 20 °C (Figure 1). This process can be repeated several times continuously on the same Lys-Cu NC system without changing the PL properties of the nanocluster. The reversible dependency of PL intensity on temperature has been primarily attributed to the conformational fluctuation of the protein scaffold. It has been hypothesized that the partial unfolding of the protein scaffold under higher temperatures exposes the nanocluster to the solvent, thereby reducing the PL intensity.[5,28,29] Similar trends can be seen for the tryptophan residues in the pure lysozyme backbone due to thermal denaturation of the protein (Figure S2).

To test this hypothesis, we exposed the Lys-Cu NC to chemical denaturants like guanidine hydrochloride (GdnHCl) or urea. These chemical denaturants can alter the scaffold conformation and can allow us to monitor the change in PL intensity of the nanoclusters, if any, due to this conformational fluctuation of the protein scaffold. It is interesting to note that the effect of the denaturant on both the scaffold (lysozyme) and the metal core can be monitored simultaneously by exciting the system at different excitation wavelengths. The lysozyme scaffold of the Lys-Cu NC can be selectively excited

https://doi.org/10.1021/acsomega.4c02223
ACS Omega 2024, 9, 21520−21527

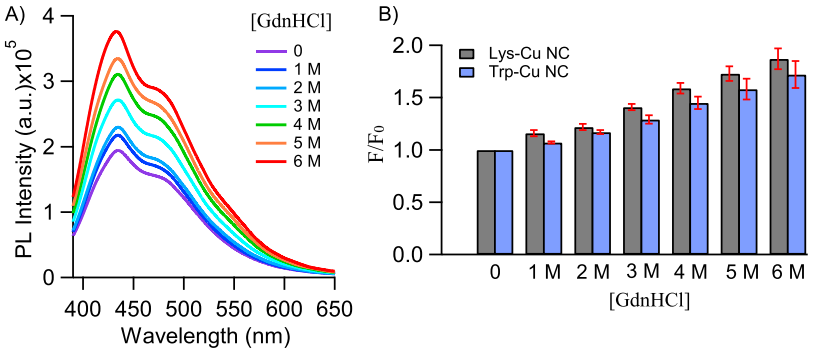

Figure 2. (A) Emission spectra of Lys-Cu NC (λ_{ex} = 365 nm) in the presence of increasing concentrations (0−6 M) of GdnHCl. (B) Ratio of PL intensities of Lys-Cu NC (λ_{ex} = 365 nm) (gray) and Trp-Cu NC (λ_{ex} = 380 nm) (blue) in the presence (F) and absence (F_0) of GdnHCl.

at 280 nm, showing an emission peak around 360 nm, corresponding to the internal tryptophan residues within the amino acid sequence of the protein carrying information on the scaffold conformation. In contrast, when excited at 365 nm, emission only from the metal core can be observed (Figure S3).

To probe the effect of scaffold conformation on the PL properties of the Lys-Cu NC, we systematically introduced an increasing concentration of GdnHCl (from 0 to 6 M) to the nanocluster solution. Surprisingly, instead of decreasing, as hypothesized from the temperature-dependent studies, the PL intensity of the nanocluster gradually increased (Figure 2A). Upon increasing the concentration of GdnHCl from 0 to 6 M, the PL intensity of the Lys-Cu NC increased by ∼1.9-fold (λ_{ex} = 365 nm) (Figure 2). To verify whether this increase in PL intensity of the Lys-Cu NC is due to the scaffold conformation, we compared the results with that of the tryptophan-capped Cu NC (Trp-Cu NC), which should not undergo any scaffold conformation-dependent change. However, interestingly, a similar trend was observed, mirroring the results seen with the Lys-Cu NC in the presence of GdnHCl (Figures 2B and S4), which suggests that the change in the PL intensity is not due to the protein conformation but most likely due to the presence of a large number of ions (Gdn^+ and Cl^-) surrounding the nanocluster. This was further confirmed by adding 6 M NaCl to the nanocluster solution, resulting in the same change, clearly suggesting that this enhancement of the PL intensity is due to the salt effect and not due to the protein conformation (Figure 3). Furthermore, the PL lifetime of the metal core of the Lys-Cu NC in the absence of any denaturant

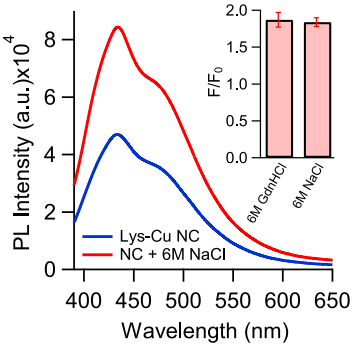

Figure 3. Emission spectra of Lys-Cu NC (λ_{ex} = 365 nm) in the absence (blue) and presence of 6 M NaCl (red). The inset shows a comparison of the change in PL intensities of the Lys-Cu NC upon the addition of 6 M GdnHCl or 6 M NaCl.

was obtained to be 2.3 ns, which remained unaffected by the presence of 6 M GdnHCl, suggesting an insignificant structural change around the metal core (Figure S5).

Further, we used a different denaturant, urea, just to check if there is any change in the effect. However, upon the addition of 10 M urea to the Lys-Cu NC solution, only a slight change (∼1.3-fold increase) in the PL intensity was observed (Figure S6). Earlier, it has been shown that though both GdnHCl and urea are structurally similar and act as a chemical denaturant their mode of action was quite different: GdnHCl usually appeared to be more efficient in denaturing proteins than urea.[44] Urea primarily exerts chaotropic effects, while GdnHCl, being a monovalent salt, encompasses both ionic and chaotropic effects.[44,45] Moreover, urea is a nonionic molecule, and therefore, it does not manifest any ionic strength effects. The addition of urea does not significantly disturb the polarity of the local environment, resulting in negligible changes in the PL intensity of the Lys-Cu NC.

Although the scaffold conformation does not seem to impart any change in the PL intensity of the metal core, it would be interesting to probe the change in the scaffold conformation in the nanocluster system in the presence of the denaturant. To gain better insights into the conformational fluctuation of the protein scaffold in the Lys-Cu NC system, the conformational change of the pure lysozyme was initially mapped by monitoring the tryptophan fluorescence signal by exciting the sample at 280 nm. When excited at 280 nm, pure lysozyme showed an emission peak around 340 nm (Figure S7). The 20 nm blue shift exhibited by the pure lysozyme in its native state compared to the lysozyme scaffold in the Lys-Cu NC system indicates that the intrinsic tryptophan residues of the pure lysozyme are partially shielded from the aqueous solvent (Figure S7).[46] The synthesis of metal nanoclusters is typically carried out at basic pH and elevated temperatures to facilitate the partial unfolding of the protein scaffold such that the active functional groups located in the protein side chains remain accessible to the nanocluster; as a result, they can coordinate and stabilize the metal core.[5,8] The protein scaffold conformation remains partially unfolded even after bringing the pH back to 7. This partially exposed tryptophan residue and its strong interaction with the metal core can explain the 20 nm shift in the emission maxima between the pure lysozyme and Lys-Cu NC (Figure S7). In the presence of the increasing concentration of GdnHCl, the PL intensity of the pure lysozyme showed a significant increase (∼4.5-fold) (Figure 4A). The addition of GdnHCl up to 3 M resulted in minimal changes, but between 3 and 6 M, a significant

https://doi.org/10.1021/acsomega.4c02223
ACS Omega 2024, 9, 21520−21527

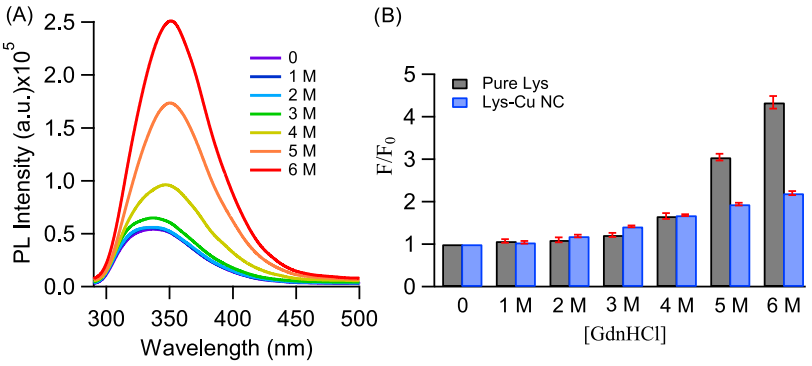

Figure 4. (A) Emission spectra of pure lysozyme (λ_{ex} = 280 nm) in the presence of increasing concentrations (0–6 M) of GdnHCl. (B) Ratio of PL intensities of pure lysozyme (λ_{ex} = 280 nm) (gray) and Lys-Cu NC (λ_{ex} = 280 nm) (blue) in the presence (F) and absence (F_0) of GdnHCl.

enhancement in the fluorescence intensity was observed along with a slight (~10 nm) red-shift in the emission maximum to 350 nm at 6 M GdnHCl, indicating the exposure of the tryptophan side chains to the solvent due to the unfolding of the protein (Figure 4A).[47]

In general, lysozymes are stable up to about 4 M GdnHCl and unfold at a higher GdnHCl concentration,[48] thus showing significant change only at a higher GdnHCl concentration. In contrast, the presence of urea did not lead to any significant changes in the photoluminescence (PL) intensity of pure lysozymes; a slight increase was observed upon the addition of 10 M urea without any change in the emission maximum (Figure S8), suggesting minimal change in the lysozyme conformation in the presence of urea. The mechanisms driving the induction of conformational changes in lysozymes by GdnHCl and urea are distinctly different.[47] Experimental findings indicate that at higher denaturant concentrations, GdnHCl can fully denature lysozymes while keeping the disulfide bonds intact, whereas urea denatures the protein only when the disulfide bonds are broken using a reducing agent; thus, GdnHCl typically appeared to be a stronger denaturing agent compared to urea.[47] This explains the inability of urea to impart any significant conformational fluctuations to the lysozyme structure.

Upon exciting the Lys-Cu NC at 280 nm in the presence of 6 M GdnHCl, only a ~2.2-fold enhancement in the PL intensity was observed without any change in the emission maxima, significantly lower than that for pure lysozymes (Figures 4B and S9). This enhancement in the PL intensity can again be attributed to the ionic strength of the medium since a similar enhancement can be observed in the presence of only 6 M NaCl (Figure S10). These results strongly suggest that the denaturant can significantly change the conformation of the pure protein in its native state but cannot alter the conformation appreciably for the protein scaffold incorporated on the surface of the NC. The partially unfolded protein scaffold stabilizes the metal core; in turn, the metal core also imparts structural stability to the partially unfolded protein scaffold, making the protein backbone more rigid.

This observation can be further confirmed by FTIR, CD, and time-resolved PL spectra. The FTIR spectra of the pure Lys and the Lys-Cu NC showed close resemblance with slight differences (Figure S11). A broad band around 3000–3500 cm^{-1} was observed in both cases due to the O–H and N–H stretching vibrations. Additionally, amide bands around 1500–1700 cm^{-1} were also evident in both cases, but a significant enhancement in intensity followed by a shoulder peak can be observed in the case of the Lys-Cu NC (Figure S11). These changes in the FTIR spectra between Lys and Lys-Cu NC could be attributed to interactions between the metal core and the functional groups of the protein backbone. Furthermore, the FTIR spectra of Lys-Cu NCs in the absence and presence of GdnHCl appeared to be fairly similar, suggesting not much change in the scaffold structure (Figure S11A). A subtle difference can be observed in the peak corresponding to the amide bands (~1500–1700 cm^{-1}) in the Lys-Cu NC: the peak slightly intensified in the presence of GdnHCl (Figure S11A). On the contrary, for pure lysozymes, a significant change can be observed, particularly around 3000–3500 cm^{-1}, corresponding to the O–H and N–H stretching vibrations upon the addition of GdnHCl due to the conformational change of the protein (Figure S11B). The CD spectra further corroborate that GdnHCl can completely disrupt the structure of pure lysozymes, but when added to the Lys-Cu NC, it did not show any significant structural alteration of the partially unfolded protein scaffold, confirming the structural stability of the protein scaffold rendered by the metal core (Figure S12).

The tryptophan residues of the pure lysozyme backbone showed an average PL lifetime of 0.5 ns, which was enhanced by ~3.3 times upon unfolding (~1.65 ns) in the presence of 6 M GdnHCl (Figure 5). Earlier, the fluorescence lifetime of the internal tryptophan residues of lysozymes was reported to be increasing when exposed to the solvent due to the decrease in energy transfer interactions with the nearby residues.[49] The average PL lifetime of a lysozyme in the Lys-Cu NC (~1.1 ns)

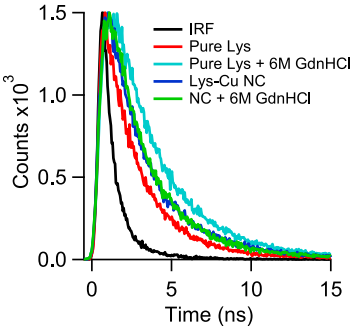

Figure 5. Time-resolved PL intensity decay profile (λ_{ex} = 280 nm; λ_{em} = 340 nm) of the pure lysozyme in the absence (red) and presence (cyan) of 6 M GdnHCl and Lys-Cu NC in the absence (blue) and presence (green) of 6 M GdnHCl. The black curve represents the instrument response function (IRF).

https://doi.org/10.1021/acsomega.4c02223
ACS Omega 2024, 9, 21520–21527

appeared to be more than that of the pure lysozyme in its native state (~0.5 ns) but less than that in the unfolded state (~1.65 ns), further confirming that the protein scaffold remains partially unfolded, slightly exposing the tryptophan while stabilizing the metal core (Figure 5). Similar to the FTIR and CD spectra, the PL lifetime of the tryptophan residues of lysozymes in the Lys-Cu NC also did not change upon the addition of 6 M GdnHCl (Figure 5), indicating a strong interaction between the lysozyme scaffold and the metal core possibly through the tryptophan residues, which remained unaffected by the denaturant. These interactions thus could play a pivotal role in providing structural stability to the protein.

The structural stability of lysozymes has significant biological implications; due to their antibacterial properties, they have been widely used as a preservative for food and beverages[50,51] as well as in wine and cheese industries to maintain the quality of products.[52,53] Their biological activity also makes them suitable for pharmaceutical and medicinal use.[51,54] In these applications, a significant challenge arises from the instability of the protein *in vitro*—isolated proteins struggling to maintain their structure and function over an extended period. Hence, the stabilization of proteins plays a key role in these applications. Earlier, osmolytes had been used as a protein stabilizer,[55] but natural osmolytes like honey could only marginally stabilize lysozymes against chemical denaturation by GdnHCl.[56] Metal nanoclusters thus could serve as an alternative for the structural stability of lysozymes and other similar amyloidogenic proteins.

Since the PL intensity of the Lys-Cu NC in the presence of chemical denaturants did not follow the trend shown by the temperature-dependent studies, the conformational fluctuation of the scaffold can be ruled out as a possible reason for the temperature-dependent PL intensity variation. Furthermore, similar thermal PL intensity fluctuation can also be observed for Trp-Cu NC (Figure S13), clearly indicating that this phenomenon is not due to the change in the surrounding environment of the nanocluster; rather, it is an intrinsic property of the metal core. Thus, the next best possible hypothesis is the enhancement in the nonradiative decay rate at the elevated temperature, resulting in the decrease in the PL intensity.[57] To test this hypothesis, we attempted to estimate the rate of radiative and nonradiative decay for the Lys-Cu NC and its temperature dependence. To evaluate the radiative and nonradiative rate constants, we measured the temperature-dependent lifetime and quantum yield of the Lys-Cu NC. The radiative rate constant at a particular temperature can be calculated from the lifetime and quantum yield of the fluorophore at that temperature using the following equation:[58,59]

$$\tau_r(T) = \frac{1}{k_r(T)} = \frac{\tau_{fl}(T)}{\phi(T)} \quad (1)$$

where $\tau_r(T)$ and $k_r(T)$ correspond to the radiative lifetime and rate constant at temperature T, respectively; $\tau_{fl}(T)$ is the measured lifetime; and $\phi(T)$ is the quantum yield of the fluorophore at temperature T. Again, the nonradiative rate constant ($k_{nr}(T)$) and lifetime ($\tau_{nr}(T)$) can be expressed as

$$k_{nr}(T) = \frac{1}{\tau_{nr}(T)} = \frac{1}{\tau_{fl}(T)} - \frac{1}{\tau_r(T)} \quad (2)$$

The quantum yield and the average lifetime of the Lys-Cu NC steadily decreased upon increasing the temperature, leading to a smaller radiative rate constant and, conversely, a larger nonradiative rate constant at an elevated temperature (Figure 6). The nonradiative rate constant increased by ~2-fold (from 36.7×10^7 s^{-1} at 25 °C to 75.6×10^7 s^{-1} at 50 °C) upon increasing the temperature from 25 to 50 °C, decreasing the overall quantum yield as well as the PL intensity of the Lys-Cu NC (Figure 6 and Table 1). Thus, this hypothesis seems to be more appropriate for explaining the temperature-dependent PL intensity variation of the Lys-Cu NC. This temperature-induced alteration of the radiative and nonradiative decay rates plays a key role in the fluorescence intensity fluctuation and thus should carefully be taken into account while studying the thermal denaturation of proteins using the internal fluorescence of tryptophan residues. By juxtaposing these perspectives, this study delves deeply into the intricate relationship between the conformation of protein scaffolds, the radiative and nonradiative relaxation rates, and the photoluminescence

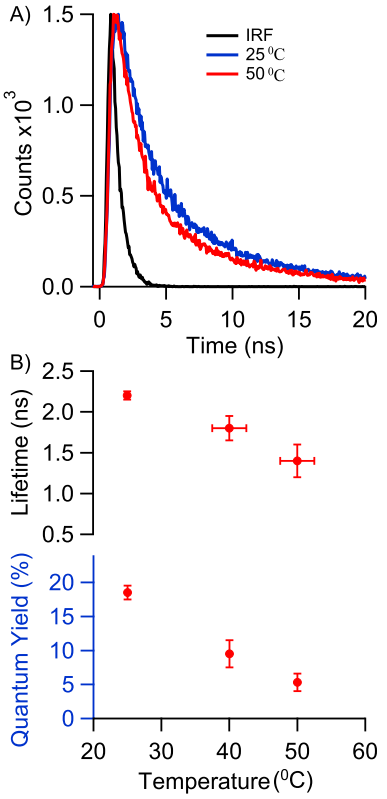

Figure 6. (A) Time-resolved PL intensity decay profile (λ_{ex} = 340 nm and λ_{em} = 437 nm) of Lys-Cu NC at 25 °C (blue) and 50 °C (red). (B) Temperature-dependent variation of the PL lifetime and quantum yield of the Lys-Cu NC.

Table 1. Temperature-Dependent PL Properties (Quantum Yield, PL Lifetime, and Radiative and Nonradiative Rate Constants) of the Lys-Cu NC

T (°C)	$\phi(T)$ (%)	$\tau_{fl}(T)$ (ns)	$k_r(T)$ (s^{-1}) × 10^7	$k_{nr}(T)$ (s^{-1}) × 10^7
25	18.5 ± 1	2.2 ± 0.05	8.3 ± 0.5	36.7 ± 0.3
40	9.5 ± 2	1.8 ± 0.15	5.5 ± 0.9	53 ± 8.6
50	5.3 ± 1.3	1.4 ± 0.2	4.2 ± 1	75.6 ± 9.5

https://doi.org/10.1021/acsomega.4c02223
ACS Omega 2024, 9, 21520−21527

intensity of metal nanoclusters, revealing profound insights into their behavior.

3. CONCLUSIONS

In summary, here, we explored the role of scaffold conformation on the luminescence properties of the metal nanocluster. Chemical denaturant-based investigation revealed a cooperative interaction between the protein scaffold and the metal core. The protein scaffold interacts and stabilizes the metal core; in turn, these interactions also make the protein backbone rigid, making the structure remain unaffected by chemical denaturants like GdnHCl. Thus, protein scaffold conformation has very little role to play in altering the PL properties of the metal core. As a result, the conformational fluctuation of the protein scaffold was ruled out as a possible reason for the temperature-induced PL intensity variation of the nanoclusters. Furthermore, small-molecule-capped metal nanoclusters (Trp-Cu NCs) also showed similar temperature-dependent PL intensity fluctuations, suggesting that this phenomenon is an inherent property of the metal core. After careful analysis, the temperature-dependent systematic variation of the radiative and nonradiative decay rates was ascribed as the key reason behind the temperature-induced PL intensity fluctuation of the Lys-Cu NC. Overall, this study strengthens the understanding of the intriguing role of scaffold conformation and the rate of nonradiative transitions on the PL properties of protein-protected metal nanoclusters.

4. MATERIALS AND METHODS

4.1. Materials. Lysozymes from hen egg white and L-tryptophan were purchased from Sisco Research Laboratories Pvt. Ltd. (SRL). Copper chloride ($CuCl_2{\cdot}2H_2O$), sodium hydroxide (NaOH), and hydrazine hydrate ($N_2H_4{\cdot}H_2O$) used for the fabrication of the nanoclusters were purchased from NICE Chemicals. Guanidine hydrochloride (GdnHCl), urea, and sodium chloride (NaCl) for examining the chemical denaturant effect on lysozymes were either purchased from SRL or NICE. All solutions were prepared using double-distilled water from the Biopak Polisher Milli-Q water system (CDUFBI001). All reagents were employed in their original state without undergoing any additional purification.

4.2. Instrumentation. Steady-state fluorescence measurements were conducted with a PerkinElmer fluorescence spectrometer (FL 8500). The Lys-Cu NC solution was excited at 365 nm, and the spectra were scanned from 390 to 650 nm at the scan rate of 240 nm min^{-1}, maintaining excitation and emission slit widths at 5 nm. Temperature-dependent fluorescence emission studies were carried out in the same instrument (FL 8500) using a Single Cell Water Jacket attached to a chiller. UV−vis absorption spectra were recorded using a Thermo Fischer Scientific (Evolution 201) UV−vis spectrophotometer. Lifetime measurements were performed on a time-correlated single-photon counting (TCSPC) setup (HORIBA, Deltaflex) using a 280 and 340 nm nano LED with an instrument response function of 1 ns. Fourier transform infrared (FTIR) spectra were captured using an IR Tracer-100 FTIR spectrometer from Shimadzu Scientific Instruments. The scanning was performed in the wavenumber range of 4700−350 cm^{-1} at 0.2 cm^{-1} resolution. The circular dichroism (CD) spectra were measured by using a Jasco J-815 spectropolarimeter. The photoluminescence quantum yield (ϕ) of the prepared nanocluster was obtained using the method reported earlier.[43]

4.3. Synthesis of Photoluminescent Lys-Cu NC and Trp-Cu NC. The lysozyme-protected copper nanocluster (Lys-Cu NC) and the tryptophan-capped copper nanocluster (Trp-Cu NC) were synthesized following a previously reported protocol.[20,43]

4.4. Effect of Denaturant on the PL Properties of the NC and the Pure Protein Scaffold. The synthesized Lys-Cu NC and Trp-Cu NC were 5-fold diluted, followed by adjusting the pH to 7. The pH of the pure lysozyme dissolved in milli-Q water was also adjusted to 7. Varying concentrations of GdnHCl (0−6 M) or urea (0−10 M) were gradually added to these solutions and incubated for 5 min. After incubation, the photoluminescence intensity (F) was recorded and compared to the intensities without any denaturant (F_0). The observed intensities were corrected for volume differences arising from the addition of GdnHCl, urea, or NaCl. All of the reported errors in this study represent the standard error of the mean (SEM) calculated from at least three or more independent measurements ($n \geq 3$).

■ ASSOCIATED CONTENT

Supporting Information

The Supporting Information is available free of charge at https://pubs.acs.org/doi/10.1021/acsomega.4c02223.

Emission spectra under different conditions, time-resolved PL intensity decay curves, FTIR spectra, and CD spectra. (PDF)

■ AUTHOR INFORMATION

Corresponding Author

Supratik Sen Mojumdar − *Department of Chemistry, Indian Institute of Technology Palakkad, Palakkad 678623 Kerala, India;* orcid.org/0000-0002-2552-1350; Email: supratik@iitpkd.ac.in

Authors

Anna Sebastian − *Department of Chemistry, Indian Institute of Technology Palakkad, Palakkad 678623 Kerala, India*

Kavya P − *Department of Chemistry, Indian Institute of Technology Palakkad, Palakkad 678623 Kerala, India*

Aarya − *Department of Chemistry, Indian Institute of Technology Palakkad, Palakkad 678623 Kerala, India*

Complete contact information is available at: https://pubs.acs.org/10.1021/acsomega.4c02223

Notes

The authors declare no competing financial interest.

■ ACKNOWLEDGMENTS

A.S. thanks CSIR. P.K. and Aarya thank UGC, Government of India, for providing fellowships. S.S.M. thanks SERB, Government of India (Project No. CRG/2022/007366), and IIT Palakkad for financial assistance. S.S.M. thanks the central instrumentation facility (CIF) at IIT Palakkad for FTIR and TCSPC measurements.

■ REFERENCES

(1) Matus, M. F.; Häkkinen, H. Understanding Ligand-Protected Noble Metal Nanoclusters at Work. *Nat. Rev. Mater.* **2023**, *8*, 372−389.

(2) Jin, R.; Zeng, C.; Zhou, M.; Chen, Y. Atomically Precise Colloidal Metal Nanoclusters and Nanoparticles: Fundamentals and Opportunities. *Chem. Rev.* **2016**, *116* (18), 10346−10413.
(3) Tao, Y.; Li, M.; Ren, J.; Qu, X. Metal Nanoclusters: Novel Probes for Diagnostic and Therapeutic Applications. *Chem. Soc. Rev.* **2015**, *44* (23), 8636−8663.
(4) Das, N. K.; Ghosh, S.; Priya, A.; Datta, S.; Mukherjee, S. Luminescent Copper Nanoclusters as a Specific Cell-Imaging Probe and a Selective Metal Ion Sensor. *J. Phys. Chem. C* **2015**, *119* (43), 24657−24664.
(5) Sebastian, A.; Aarya; Sarangi, B. R.; Sen Mojumdar, S. Lysozyme Protected Copper Nano-Cluster: A Photo-Switch for the Selective Sensing of Fe2+. *J. Photochem. Photobiol. A* **2023**, *436*, No. 114378.
(6) Chen, P.-C.; Li, Y.-C.; Ma, J.-Y.; Huang, J.-Y.; Chen, C.-F.; Chang, H.-T. Size-Tunable Copper Nanocluster Aggregates and Their Application in Hydrogen Sulfide Sensing on Paper-Based Devices. *Sci. Rep.* **2016**, *6* (1), No. 24882.
(7) Xu, H.; Suslick, K. S. Water-Soluble Fluorescent Silver Nanoclusters. *Adv. Mater.* **2010**, *22* (10), 1078−1082.
(8) Ghosh, S.; Das, N. K.; Anand, U.; Mukherjee, S. Photostable Copper Nanoclusters: Compatible Förster Resonance Energy-Transfer Assays and a Nanothermometer. *J. Phys. Chem. Lett.* **2015**, *6* (7), 1293−1298.
(9) Derfus, A. M.; Chan, W. C. W.; Bhatia, S. N. Probing the Cytotoxicity Of Semiconductor Quantum Dots. *Nano Lett.* **2004**, *4* (1), 11−18.
(10) Resch-Genger, U.; Grabolle, M.; Cavaliere-Jaricot, S.; Nitschke, R.; Nann, T. Quantum Dots versus Organic Dyes as Fluorescent Labels. *Nat. Methods* **2008**, *5* (9), 763−775.
(11) Fang, J.; Zhang, B.; Yao, Q.; Yang, Y.; Xie, J.; Yan, N. Recent Advances in the Synthesis and Catalytic Applications of Ligand-Protected, Atomically Precise Metal Nanoclusters. *Coord. Chem. Rev.* **2016**, *322*, 1−29.
(12) Wilcoxon, J. P.; Abrams, B. L. Synthesis, Structure and Properties of Metal Nanoclusters. *Chem. Soc. Rev.* **2006**, *35* (11), 1162−1194.
(13) Chakraborty, S.; Mukherjee, S. Effects of Protecting Groups on Luminescent Metal Nanoclusters: Spectroscopic Signatures and Applications. *Chem. Commun.* **2021**, *58* (1), 29−47.
(14) Li, H.; Huang, H.; Feng, J.-J.; Luo, X.; Fang, K.-M.; Wang, Z.-G.; Wang, A.-J. A Polypeptide-Mediated Synthesis of Green Fluorescent Gold Nanoclusters for Fe3+ Sensing and Bioimaging. *J. Colloid Interface Sci.* **2017**, *506*, 386−392.
(15) Hu, Y.; Guo, W.; Wei, H. Protein- and Peptide-directed Approaches to Fluorescent Metal Nanoclusters. *Isr. J. Chem.* **2015**, *55* (6−7), 682−697.
(16) Liu, J. DNA-Stabilized, Fluorescent, Metal Nanoclusters for Biosensor Development. *TrAC, Trends Anal. Chem.* **2014**, *58*, 99−111.
(17) Ding, Y.; Li, X.; Chen, C.; Ling, J.; Li, W.; Guo, Y.; Yan, J.; Zha, L.; Cai, J. A Rapid Evaluation of Acute Hydrogen Sulfide Poisoning in Blood Based on DNA-Cu/Ag Nanocluster Fluorescence Probe. *Sci. Rep.* **2017**, *7* (1), No. 9638.
(18) Xu, H.; Suslick, K. S. Sonochemical Synthesis of Highly Fluorescent Ag Nanoclusters. *ACS Nano* **2010**, *4* (6), 3209−3214.
(19) Tanaka, S.-I.; Miyazaki, J.; Tiwari, D. K.; Jin, T.; Inouye, Y. Fluorescent Platinum Nanoclusters: Synthesis, Purification, Characterization, and Application to Bioimaging. *Angew. Chem., Int. Ed.* **2011**, *50* (2), 431−435.
(20) Aarya; Thomas, T.; Sarangi, B. R.; Sen Mojumdar, S. Rapid Detection of Ag(I) via Size-Induced Photoluminescence Quenching of Biocompatible Green-Emitting, L -Tryptophan-Scaffolded Copper Nanoclusters. *ACS Omega* **2023**, *8* (16), 14630−14640.
(21) Liu, Y.; Ding, D.; Zhen, Y.; Guo, R. Amino Acid-Mediated 'Turn-off/Turn-on' Nanozyme Activity of Gold Nanoclusters for Sensitive and Selective Detection of Copper Ions and Histidine. *Biosens. Bioelectron.* **2017**, *92*, 140−146.
(22) Kavya, P.; Aarya; Sebastian, A.; Sen Mojumdar, S. L-Tyrosine Capped Silver Nanocluster: An Efficient Reusable Luminescent Nano-Probe for Simple, Rapid and Reliable Detection of Hemoglobin in Real Blood Samples. *Sens. Actuators, B* **2024**, *401*, No. 134923.
(23) Anand, U.; Ghosh, S.; Mukherjee, S. Toggling Between Blue- and Red-Emitting Fluorescent Silver Nanoclusters. *J. Phys. Chem. Lett.* **2012**, *3* (23), 3605−3609.
(24) Chib, R.; Butler, S.; Raut, S.; Shah, S.; Borejdo, J.; Gryczynski, Z.; Gryczynski, I. Effect of Quencher, Denaturants, Temperature and pH on the Fluorescent Properties of BSA Protected Gold Nanoclusters. *J. Lumin.* **2015**, *168*, 62−68.
(25) Wu, Y.-T.; Shanmugam, C.; Tseng, W.-B.; Hiseh, M.-M.; Tseng, W.-L. A Gold Nanocluster-Based Fluorescent Probe for Simultaneous pH and Temperature Sensing and Its Application to Cellular Imaging and Logic Gates. *Nanoscale* **2016**, *8* (21), 11210−11216.
(26) Chen, X.; Essner, J. B.; Baker, G. A. Exploring Luminescence-Based Temperature Sensing Using Protein-Passivated Gold Nanoclusters. *Nanoscale* **2014**, *6* (16), 9594−9598.
(27) Zhang, L.; Zhang, M.; Wu, Y. Temperature-Induced Optical Property and Conformational Change of BSA-Protected Gold Nanoclusters. *J. Mol. Struct.* **2014**, *1069*, 245−250.
(28) Esquembre, R.; Sanz, J.; Wall, J. G.; del Monte, F.; Mateo, C. R.; Ferrer, M. L. Thermal Unfolding and Refolding of Lysozyme in Deep Eutectic Solvents and Their Aqueous Dilutions. *Phys. Chem. Chem. Phys.* **2013**, *15* (27), 11248−11256.
(29) Knubovets, T.; Osterhout, J. J.; Connolly, P. J.; Klibanov, A. M. Structure, Thermostability, and Conformational Flexibility of Hen Egg-White Lysozyme Dissolved in Glycerol. *Proc. Natl. Acad. Sci. U.S.A.* **1999**, *96* (4), 1262−1267.
(30) Robertson, A. D.; Murphy, K. P. Protein Structure and the Energetics of Protein Stability. *Chem. Rev.* **1997**, *97* (5), 1251−1268.
(31) Xiong, H.; Wang, W.; Liang, J.; Wen, W.; Zhang, X.; Wang, S. A Convenient Purification Method for Metal Nanoclusters Based on pH-Induced Aggregation and Cyclic Regeneration and Its Applications in Fluorescent pH Sensors. *Sens. Actuators, B* **2017**, *239*, 988−992.
(32) Pandit, S.; Kundu, S. pH-Dependent Reversible Emission Behaviour of Lysozyme Coated Fluorescent Copper Nanoclusters. *J. Lumin.* **2020**, *228*, No. 117607.
(33) Wang, C.; Wang, C.; Xu, L.; Cheng, H.; Lin, Q.; Zhang, C. Protein-Directed Synthesis of pH-Responsive Red Fluorescent Copper Nanoclusters and Their Applications in Cellular Imaging and Catalysis. *Nanoscale* **2014**, *6* (3), 1775−1781.
(34) Wang, W.; Leng, F.; Zhan, L.; Chang, Y.; Yang, X. X.; Lan, J.; Huang, C. Z. One-Step Prepared Fluorescent Copper Nanoclusters for Reversible pH-Sensing. *Analyst* **2014**, *139* (12), 2990−2993.
(35) Xiaoqing, L.; Ruiyi, L.; Xiaohuan, L.; Zaijun, L. Ultra Sensitive and Wide-Range pH Sensor Based on the BSA-Capped Cu Nanoclusters Fabricated by Fast Synthesis through the Use of Hydrogen Peroxide Additive. *RSC Adv.* **2015**, *5* (60), 48835−48841.
(36) Jia, Y.; Sun, T.; Jiang, Y.; Sun, W.; Zhao, Y.; Xin, J.; Hou, Y.; Yang, W. Green, Fast, and Large-Scale Synthesis of Highly Fluorescent Au Nanoclusters for Cu 2+ Detection and Temperature Sensing. *Analyst* **2018**, *143* (21), 5145−5150.
(37) Cai, Z.-f.; Li, H.; Wang, X.; Min, C.; Wen, J.; Fu, R.; Dai, Z.; Chen, J.; Guo, M.; Yang, H.; Bai, P.; Lu, X.; Wu, T.; Wu, Y. Highly Luminescent Copper Nanoclusters as Temperature Sensors and "Turn off" Detection of Oxytetracycline. *Colloids Surf., A* **2022**, *647*, No. 129202.
(38) Deng, H.-H.; Wu, G.-W.; Zou, Z.-Q.; Peng, H.-P.; Liu, A.-L.; Lin, X.-H.; Xia, X.-H.; Chen, W. pH-Sensitive Gold Nanoclusters: Preparation and Analytical Applications for Urea, Urease, and Urease Inhibitor Detection. *Chem. Commun.* **2015**, *51* (37), 7847−7850.
(39) Huang, H.; Li, H.; Feng, J.-J.; Wang, A.-J. One-Step Green Synthesis of Fluorescent Bimetallic Au/Ag Nanoclusters for Temperature Sensing and in Vitro Detection of Fe3+. *Sens. Actuators, B* **2016**, *223*, 550−556.
(40) Wang, C.; Cheng, H.; Huang, Y.; Xu, Z.; Lin, H.; Zhang, C. Facile Sonochemical Synthesis of pH-Responsive Copper Nano-

https://doi.org/10.1021/acsomega.4c02223
ACS Omega 2024, 9, 21520−21527

clusters for Selective and Sensitive Detection of Pb2+ in Living Cells. *Analyst* **2015**, *140* (16), 5634−5639.
(41) Sułkowska, A.; Równicka, J.; Bojko, B.; Pożycka, J.; Zubik-Skupień, I.; Sułkowski, W. Effect of Guanidine Hydrochloride on Bovine Serum Albumin Complex with Antithyroid Drugs: Fluorescence Study. *J. Mol. Struct.* **2004**, *704* (1−3), 291−295.
(42) Monera, O. D.; Kay, C. M.; Hodges, R. S. Protein Denaturation with Guanidine Hydrochloride or Urea Provides a Different Estimate of Stability Depending on the Contributions of Electrostatic Interactions. *Protein Sci.* **1994**, *3* (11), 1984−1991.
(43) Sebastian, A.; Aarya; Kavya, P.; Sen Mojumdar, S. Role of a Mild Reducing Agent in Designing a Copper Nanocluster-Based Tunable Dual-Metal Sensor for the Selective and Sensitive Detection of Ag+ and Fe2+. *Chem. Phys. Impacts* **2023**, *6*, No. 100249.
(44) Lim, W. K.; Rösgen, J.; Englander, S. W. Urea, but Not Guanidinium, Destabilizes Proteins by Forming Hydrogen Bonds to the Peptide Group. *Proc. Natl. Acad. Sci. U.S.A.* **2009**, *106* (8), 2595−2600.
(45) Rashid, F.; Sharma, S.; Bano, B. Comparison of Guanidine Hydrochloride (GdnHCl) and Urea Denaturation on Inactivation and Unfolding of Human Placental Cystatin (HPC). *Protein J.* **2005**, *24* (5), 283−292.
(46) West, S. M.; Guise, A. D.; Chaudhuri, J. B. A Comparison of the Denaturants Urea and Guanidine Hydrochloride on Protein Refolding. *Food Bioprod. Process.* **1997**, *75* (1), 50−56.
(47) Biswas, B.; Muttathukattil, A. N.; Reddy, G.; Singh, P. C. Contrasting Effects of Guanidinium Chloride and Urea on the Activity and Unfolding of Lysozyme. *ACS Omega* **2018**, *3* (10), 14119−14126.
(48) Emadi, S.; Behzadi, M. A Comparative Study on the Aggregating Effects of Guanidine Thiocyanate, Guanidine Hydrochloride and Urea on Lysozyme Aggregation. *Biochem. Biophys. Res. Commun.* **2014**, *450* (4), 1339−1344.
(49) Rmoso, C.; Forster, L. S. Tryptophan Fluorescence Lifetimes in Lysozyme. *J. Biol. Chem.* **1975**, *250* (10), 3738−3745.
(50) Nawaz, N.; Wen, S.; Wang, F.; Nawaz, S.; Raza, J.; Iftikhar, M.; Usman, M. Lysozyme and Its Application as Antibacterial Agent in Food Industry. *Molecules* **2022**, *27* (19), 6305.
(51) Proctor, V. A.; Cunningham, F. E.; Fung, D. Y. C. The Chemistry of Lysozyme and Its Use as a Food Preservative and a Pharmaceutical. *CRC Crit. Rev. Food Sci. Nutr.* **1988**, *26* (4), 359−395.
(52) Delfini, C.; Cersosimo, M.; Del Prete, V.; Strano, M.; Gaetano, G.; Pagliara, A.; Ambrò, S. Resistance Screening Essay of Wine Lactic Acid Bacteria on Lysozyme: Efficacy of Lysozyme in Unclarified Grape Musts. *J. Agric. Food Chem.* **2004**, *52* (7), 1861−1866.
(53) Schneider, N.; Werkmeister, K.; Becker, C.-M.; Pischetsrieder, M. Prevalence and Stability of Lysozyme in Cheese. *Food Chem.* **2011**, *128* (1), 145−151.
(54) Ferraboschi, P.; Ciceri, S.; Grisenti, P. Applications of Lysozyme, an Innate Immune Defense Factor, as an Alternative Antibiotic. *Antibiotics* **2021**, *10* (12), 1534.
(55) Street, T. O.; Bolen, D. W.; Rose, G. D. A Molecular Mechanism for Osmolyte-Induced Protein Stability. *Proc. Natl. Acad. Sci. U.S.A.* **2006**, *103* (38), 13997−14002.
(56) Wong, Y. H.; Lim, C. H.; Kadir, H. A.; Tayyab, S. Towards Increasing Chemical and Thermal Stability of Lysozyme with a Simulated Honey Sugar Cocktail. *RSC Adv.* **2014**, *4* (96), 53891−53898.
(57) Wang, C.; Lin, H.; Xu, Z.; Huang, Y.; Humphrey, M. G.; Zhang, C. Tunable Carbon-Dot-Based Dual-Emission Fluorescent Nanohybrids for Ratiometric Optical Thermometry in Living Cells. *ACS Appl. Mater. Interfaces* **2016**, *8* (10), 6621−6628.
(58) Omogo, B.; Aldana, J. F.; Heyes, C. D. Radiative and Non-Radiative Lifetime Engineering of Quantum Dots in Multiple Solvents by Surface Atom Stoichiometry and Ligands. *J. Phys. Chem. C* **2013**, *117* (5), 2317−2327.
(59) Shirakov, A.; Burshtein, Z.; Shimony, Y.; Frumker, E.; Ishaaya, A. A. Radiative and Non-Radiative Transitions of Excited Ti3+ Cations in Sapphire. *Sci. Rep.* **2019**, *9*, No. 18810.

https://doi.org/10.1021/acsomega.4c02223
ACS Omega 2024, 9, 21520−21527